Eighth Australasian Fluid Mechanics Conference, University of Newcastle, N.S.W., 28 November/2 December 1983.

CONTACT ZONE INSTABILITY DUE TO REAL GAS EFFECTS IN SHOCK TUBE FLOWS

A.F.P. HOUWING AND R.J. SANDEMAN

DEPARTMENT OF PHYSICS

AUSTRALIAN NATIONAL UNIVERSITY, CANBERRA, A.C.T. 2600 AUSTRALIA

SUMMARY A simple theory is presented to describe the motion of a non-ideal contact surface, or mixing front, during shock tube flow. Under certain conditions, this mixing front is predicted to become trapped within the relaxation zone, and thus destroy shock planarity. Under other conditions, the interaction of the mixing front with the sidewall boundary layer is considered to be responsible for reducing the length of the test sample below that predicted for ideal behaviour. The theory compares well with experiments when variations in the mean molecular weight of the test gas are small.

1. INTRODUCTION

Work by earlier investigators has shown that the homogeneity of test samples in shock tube flow can be destroyed by contamination with the driver gas. Levine (1970) investigated this problem in helium-argon test gas mixtures with a helium driver, in order to explore the role of the average molecular weight on the formation of the test sample. His results were correlated with a theory, that supposed a turbulent mixing region, instead of an infinitely thin contact surface. The analysis predicted that certain mixtures generated in this region were buoyant in the pseudo-gravitational field produced by the ionization of argon behind the shock. These buoyant mixtures were assumed to form an interface, termed the mixing front, which was able to perturb the flow behind the shock front. Houwing, Hornung and Sandeman (1981) have demonstrated the existence of this mixing front in shock tube experiments using sulphur hexafluoride as the test gas. However their results revealed discrepancies between Levine's predictions and their observations. The present work seeks to reconcile these discrepancies by re-deriving the equation of motion for the mixing front and comparing the predictions with new experiments in sulphur hexafluoride, carbon dioxide and argon.

2. THEORY

Consider the motion of a particle of mass M and velocity u_b in a frictionless accelerating fluid of velocity u_2. Batchelor (1967) shows that if the particle is assumed to be a non-deforming sphere, then

$$M \frac{du_b}{dt} = M_0 \frac{du_2}{dt} - \frac{1}{2} M_0 \frac{d(u_b-u_2)}{dt}, \qquad (1)$$

where M_0 is the mass of the fluid displaced. If we define

$$R = M_0/M = \rho_2/\rho_m , \qquad (2)$$

where ρ_m is the density of the particle and ρ_2 that of the surrounding fluid, then equation (1) can be reduced to give

$$du_b = \frac{3R}{2+R} du_2 . \qquad (3)$$

We assume that the particle, whose motion is described by equation (3), is typical of the large number of particles which make up the mixing front. Consequently, in the shock-fixed reference frame, u_b is the velocity of the mixing front and u_2 that of the gas between it and the shock wave. The density of the test gas then is ρ_2, while that of the mixture directly behind the mixing front is ρ_m. If we assume R to be constant and integrate equation (3), we obtain

$$u_b(x) = \frac{3R}{2+R} u_2(x) + \frac{2-2R}{2+R} u_2(0), \qquad (4)$$

where the boundary condition is that the test gas and mixing front have equal velocities at x=0, this corresponding to conditions directly after rupture of the shock tube diaphragm. We consider the case where the test gas velocity decreases monatomically with x, this variation being the result of either non-equilibrium effects behind the shock or mass entrainment through the side wall boundary layer. The mixing front is considered to be coincident with the shock (i.e. at x=0) directly after diaphragm rupture, and to separate from it as it travels along the shock tube. Since the test gas velocity $u_2(x)$ is decreasing, equation (4) predicts the velocity $u_b(x)$ of the mixing front to also decrease. Furthermore, equation (4) predicts $u_b = 0$, at a particular value of $x = \ell_m^*$, when

$$u_2(\ell_m^*) = \frac{2}{3} (1 - 1/R) u_2(0) \qquad (5)$$

The value ℓ_m^* is therefore the maximum separation of the mixing front from the shock and corresponds to the value of x for which the mixing front is stationary with respect to the shock wave.

2.1 The effect of relaxation

We consider firstly the effect of relaxation on the value of ℓ_m^*. For a shock wave with a relaxation length x_r, the mixing front will become trapped inside the relaxation zone behind the shock, if

$$0 < \ell_m^* < x_r \qquad (6)$$

For non-equilibrium processes relevant to the present investigation, the value of $u_2(x)$ decreases monatomically from u_{2f} to u_{2e}, viz.

$$u_{2e} = u_2(x_r) < u_2(x) < u_2(0) = u_{2f}, \qquad (7)$$

where the subscripts f and e refer to frozen and equilibrium conditions, respectively. Thus, inequality (6) can only be satisfied if

$$H \equiv \frac{2}{3} (1 - 1/R) \frac{\rho_{2e}}{\rho_{2f}} > 1. \qquad (8)$$

Levine, on the other hand, predicts that the condition in inequality (6) is satisfied when

$$L^2 \equiv (R-1) \left[\left(\frac{\rho_{2e}}{\rho_{2f}} \right)^2 - 1 \right] > 1. \qquad (9)$$

It is important to note that relaxation effects will cause variations in ρ_2, from which one must expect that R may also vary.[2] However, if ρ_m is calculated

in the same manner as that suggested by Levine (who proposes isobaric adiabatic mixing of the driver and test gases) then R is approximately equal to the ratio of average molecular weights across the mixing front. This implies that R will be a constant for vibrational non-equilibrium, but can vary significantly if dissociation or ionization becomes important. Since R has been assumed to be a constant in the integration of equation (3), the inequality (8) is only an approximate criterion for trapping of the mixing front for these latter cases.

2.2 The effect of mass entrainment

For the case of sidewall boundary layer entrainment, the theory of Mirels (1964) considers the boundary layer profiles to be independent of variations in the inviscid core. He shows that the velocity profile behind a normal shock in the presence of a sidewall boundary layer is given by

$$u_2(x) = u_2(0)\left[1 - \left(\frac{x}{\ell_m}\right)^{1-n}\right], \qquad (10)$$

where ℓ_m is the maximum separation of an ideal contact surface from the shock, n = 1/2 for a laminar boundary layer and n = 1/5 for the turbulent case. If x_r is small compared to ℓ_m, then we may assume that $u_2(0) = u_{2e}$ and substitute equation (10) into (4) to give

$$u_b(x) = u_{2e}\left[1 - \frac{3R}{2+R}\left(\frac{x}{\ell_m}\right)^{1-n}\right]. \qquad (11)$$

Equation (11) predicts u_b to equal zero and hence the mixing front to reach its maximum separation when

$$x = \ell_m^* = \ell_m\left[\frac{2+R}{3R}\right]^{\frac{1}{1-n}}. \qquad (12)$$

The separation ℓ of the ideal contact surface as an implicit function of time t elapsed since diaphragm rupture was determined by Mirels by putting $u_2 = d\ell/dt$ into equation (10). The same can be done here for the mixing front by denoting its separation by ℓ^* and putting $u_b = d\ell^*/dt$ into equation (11). This equation can then be integrated to give

$$-T/2 = \ln(1-X^n) + X^n, \text{ for } n = 1/2 \qquad (13)$$

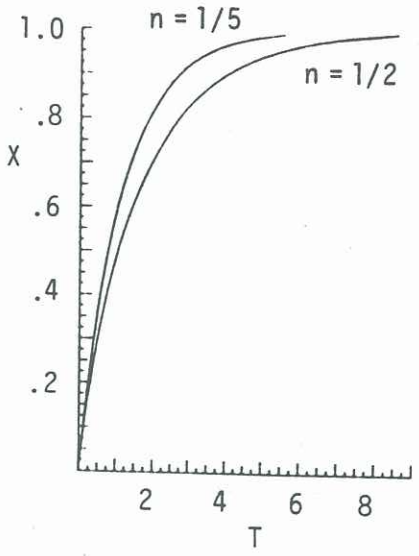

Figure 1. Similarity solutions for test sample length

$$-T/2 = \frac{5}{8}\left[\ln\frac{1-X^n}{1+X^n} - 2\tan^{-1}X^n + 4X^n\right], \text{ for } n = 1/5 \qquad (14)$$

where

$$T = \frac{u_{2e}t}{\ell_m}\left(\frac{3R}{2+R}\right)^{\frac{1}{1-n}}, \qquad (15)$$

$$X = \frac{\ell^*}{\ell_m}\left(\frac{3R}{2+R}\right)^{\frac{1}{1-n}}. \qquad (16)$$

This is identical to the Mirels' result when R=1. A plot of X as a function of T is given in figure 1 for the two types of boundary layer. Note that for T > 5, X ≈ 1, and therefore $\ell^* \simeq \ell_m^*$. In the experiments to be discussed here T > 50, and therefore the mixing front is expected to be at its maximum separation ℓ_m^*.

3. EXPERIMENT

Shock waves and mixing fronts in carbon dioxide, argon and mixtures of SF_6 and argon were observed using

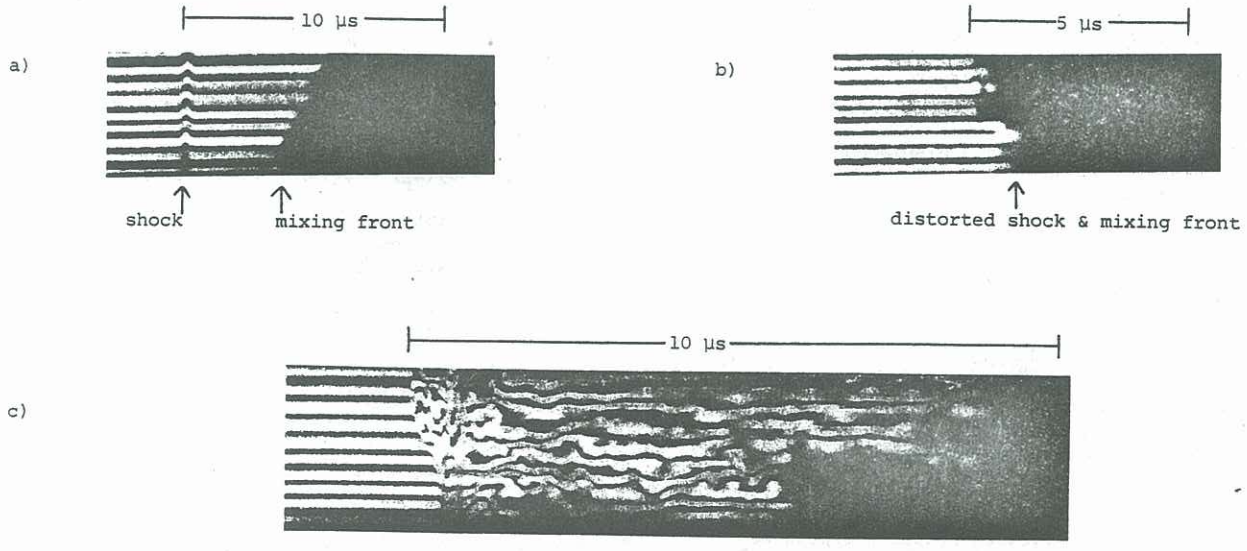

Figure 2. (a) undistorted shock, (b) and (c) distorted shocks.

the experimental arrangement described by Houwing et al. (1981). However, under certain conditions, differential interferometry was used to observe the shock and a new spectral line absorption method to detect the mixing front. This method consisted of introducing sodium into the driver gas in the form of salt. During the diaphragm rupture process associated with the operation of a free piston shock tube, the salt mixes with the heated driver gas and dissociates to form sodium metal vapour. After diaphragm rupture, this metal vapour is carried into the shock tube with the driver gas. Similar impurities on the shock tube wall are not expected to be as readily introduced into the flow, since they are expected to remain trapped within the cooler boundary layer in the form of salts. Thus if a laser beam, which is tuned to the D2 resonance transition of sodium (588.96 nm), transverses the test section and the transmission monitored by a photodiode, negligible absorption is expected in the test sample but appreciable absorption is expected behind the mixing front. In order to synchronise this method with the flow interferometry, an argon-ion pumped ring-dye-laser, tuned to the D2 line, was used as the light source for the differential interferometer. This gave clear visualization of the mixing zone and allowed accurate measurements of test sample lengths at low test gas densities, where conventional flow interferometry was not sufficiently sensitive to detect the mixing front. However, the method was not used for shock waves in mixtures of SF_6 and argon, for which the shadowgraph method used by Houwing et al. was sufficiently sensitive to detect the mixing front.

Undistorted and distorted shocks are presented in figure 2, which shows interferograms obtained with the spectrally tuned interferometer. In figure 2(a) the mixing front is separated from a plane shock, while in 2(b) the mixing front is coincident with the shock and we suggest that it is trapped within the relaxation zone. Figure 2(c) illustrates a badly perturbed mixing front with long tongue-like projections which extend into the test sample. Although the main body of the mixing zone appears to be well separated from the shock front, these projections appear to be responsible for the disturbance at the shock. Thus the shock distortion in this instance was classed as being a result of the contact zone instability. However, under other conditions, shock waves were found to be distorted even when they appeared to be unaffected by conditions in the contact zone. These were classed as being inherently unstable and are discussed in further detail by Houwing and Sandeman (1983).

4. RESULTS AND CONCLUSIONS

In order to compare the experimental observations with the predictions of Levine and those of the present work, the parameters R, L and H were evaluated and plotted in figure 3. Equilibrium shock jump conditions were calculated using the published data of McBride et al. (1963), Simcox and Peterson (1965) and Chase et al. (1978). The experiments with SF_6 were sufficiently far from the conditions for liquefaction behind the shock wave (Dettleff et al., 1979) to ignore intermolecular forces. The methods of Levine (1970) and Houwing et al. (1981) were used to determine the value of R. For the SF_6-Ar experiments for which most of the non-equilibrium effects were due to vibrational relaxation, it was found that the average molecular weight at equilibrium was sufficiently close to the frozen value to satisfy the assumption of constant R. However, this was not the case for experiments in dissociating carbon dioxide or ionizing argon.

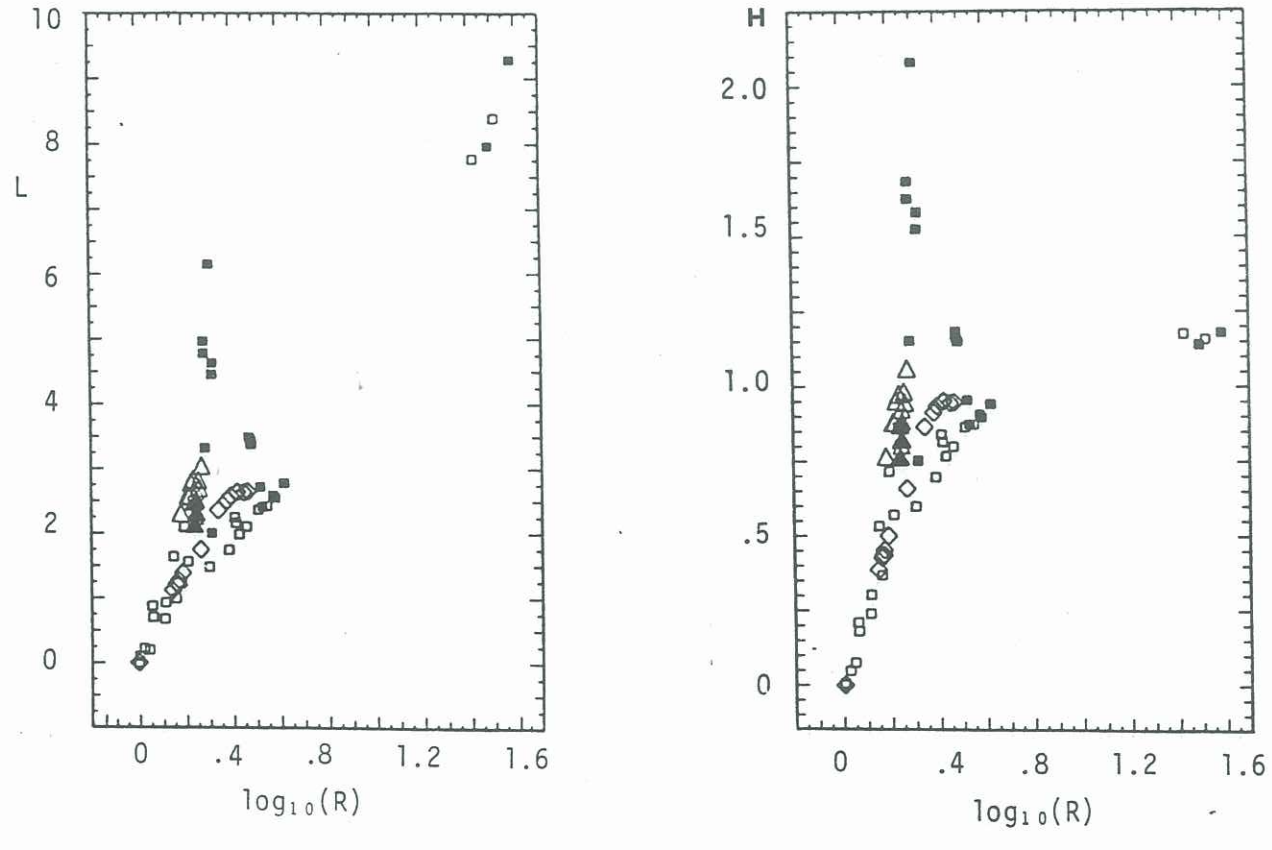

(a) Levine's model

(b) Present model

Figure 3. The stability parameters. Filled symbols indicate instability. △- Ar; ◇- CO_2; □ - SF_6/Ar.

and thus the calculations of R, L and H for these experiments must be regarded as crude estimates. From figure 3, it is readily seen that correlation with Levine's parameter is poor, with unperturbed shocks being observed for L >> 1. On the other hand, good correlation is achieved with the parameter H, suggesting that the present approach is more accurate.

When H << 1 and the similarity assumptions of Mirels (1964) are satisfied, the maximum separation of the mixing front from the shock is given by equation (12). We have calculated the Reynolds number from Mirels' (1956) formulae and compared the values to the data of Hartunian et al. (1960), from which we found that it was valid to assume a turbulent boundary layer for the SF_6-Ar experiments. Consequently, the value of ℓ_m was calculated from Mirels' (1956, 1964) formulae with n = 1/5. The resulting values for ℓ_m and ℓ_m^* together with the experimentally measured separation distance Δ are presented in figure 4. This shows that equation (12) correctly predicts the test sample length. We consider therefore that discrepancies between Mirels' predictions and experimental measurements can be explained in terms of a simple model of bouyant mixing of the driver and test gases. However the similarity assumptions are no longer valid for dissociating and ionizing flow. In fact, Liu et al. (1980) demonstrate that in ionizing argon the boundary layer and the free stream are strongly coupled. For this reason, values of ℓ_m^* for dissociating carbon dioxide or ionizing argon are not included in figure 4.

5. CONCLUDING REMARKS

It is important to note that in the experiments for dissociating and ionizing gases, the temperature of the test gas is much higher than that of the driver gas. However, for the case of vibrational relaxation, these temperatures are almost equal. One is justified therefore in using equations (8) and (12) for the SF_6-Ar experiments, but not so for the remaining experiments for which heat transfer across the mixing front is expected to be appreciable. This, together with the fact that the average molecular weight can change appreciably through the relaxation zone, makes it necessary to develop a more sophisticated model for these cases. Such a model, which will also remove the similarity assumptions by incorporating the method of Liu et al. (1980), is presently under consideration.

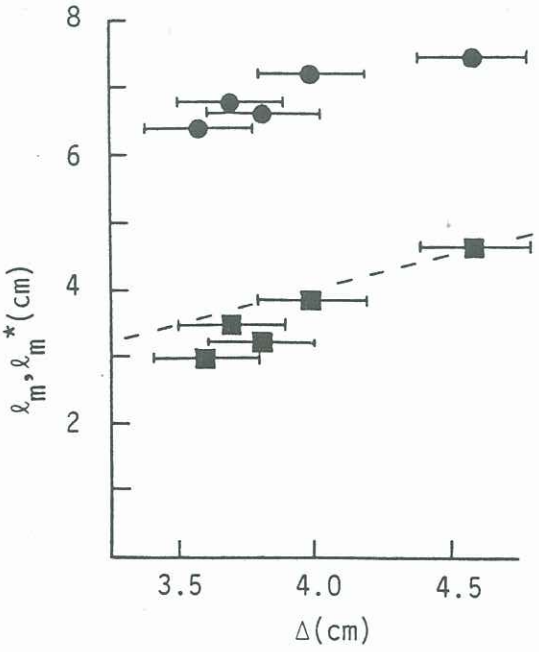

Figure 4. Test sample lengths.
● - ℓ_m; ■ - ℓ_m^*

6. REFERENCES

BATCHELOR, G.K. (1974) An Introduction to fluid dynamics, Cambridge University Press, 454.

CHASE, M.W., CURNUTT, J.L., McDONALD, R.A. & SYVERUD, A.N. (1978) JANAF thermochemical tables, 1978 Supplement. J. Phys. Chem. Ref. Data 7 (3), 793-940.

DETTLEFF, G., THOMPSON, P.A., MEIER, G.E.A. & SPECKMANN, H.D. (1979) An experimental study of liquefaction shock waves. J. Fluid Mech. 95 (2), 297-304.

HARTUNIAN, R., RUSSO, A. & MARRONE, P. (1960) Boundary layer transition and heat transfer in shock tubes. J. Aerospace Sci. 27, 587-594.

HOUWING, A.F.P., HORNUNG, H.G. & SANDEMAN, R.J. (1981) Investigation of the distortion of shock fronts in real gases. Proc. 13th Int. Sym. Shock Tubes & Waves, Niagara Falls, 176-184.

HOUWING, A.F.P. & SANDEMAN, R.J. (1983) Shock wave instability and spontaneous acoustic emission for arbitrary disturbances in real gases. Proc. 8th Austral. Hydr. Fluid Mech. Conf., Newcastle.

LEVINE, M.A. (1970) Turbulent mixing at the contact surface in a driven shock wave. Phys. Fluids 13, 1166-1171.

LIU, W.S., TAKAYAMA, K. & GLASS, I.I. (1980) Coupled interactions of shock wave structure with laminar boundary layers in ionizing-argon flows, J. Fluid Mech. 97 (3), 513-530.

McBRIDE, F.J., HEIMELS, S., EHLERS, J.G. & GORDON, S. (1963) Thermodynamic properties to 6000 °K for 210 substances involving the first 18 elements, NASA SP-3001.

MIRELS, H. (1956) Boundary layer behind shock or thin expansion wave moving into stationary fluid, NACA TN 3712.

MIRELS, H. (1964) Shock tube test time limitation due to turbulent-wall boundary layer, AIAA J. 2, 84-92.

SIMCOX, C.D. & PETERSON, V.L. (1965) Charts for equilibrium and frozen flows across plane shock waves in carbon dioxide, NASA SP-3018.